Austenitic Stainless Steel–Ferritic Steel Weld Joint Failures

Recommendations for extending weld joint lifetime include using transition pieces with intermediate coefficients of thermal expansion between the two steels and using transition pieces that minimize carbon transfer

BY R. L. KLUEH AND J. F. KING

ABSTRACT. The cause of failures of dissimilar-alloy (austenitic or ferritic) joints in superheater and reheater tubes of fossil-fired steam plants was investigated. In the failures of interest, cracks form and propagate in the ferritic steel (usually 2¼ Cr-1 Mo steel) about 5 to 15 μm from the fusion line. The complex microstructure developed at the interface between weld metal and 2¼ Cr-1 Mo steel during welding and elevated-temperature service was examined in (1) the as-welded and as-welded-and-tempered conditions and (2) failed and unfailed joints having more than 100,000 h of service in a fossil-fired boiler.

Metallographic observations on failed and unfailed joints were combined with literature observations to explain the interface microstructure and subsequent failure mode. On the basis of the proposed failure model, recommendations are presented for improving joint reliability.

Introduction

Since the 1940's, both ferritic heat-resisting steels and austenitic stainless steels have been used in most commercial fossil-fired power plants. Primary boilers and heat exchangers operate at temperatures and environmental conditions that make low-alloy ferritic steels the best choice for the structural material. The chromium-molybdenum steels—especially 2¼ Cr-1 Mo steel—have been used extensively. For the superheater, reheater tubes, headers, and the hot-reheat steam pipes, however, the elevated temperatures usually make austenitic stainless steels the necessary choice. Because of this use of two materials within one system, a transition joint is required.

The problems inherent in such joints have long been recognized (Ref. 1-5). The utility industry has experienced a rash of transition-joint failures in fossil-fired steam plants. These failures often occur after 15 to 20 years of operation, well before the lifetime of the tubing is exhausted. Because of the economic consequences of a power plant shutdown, the need for an improved dissimilar alloy weld is obvious.

Nearly all austenitic-ferritic, dissimilar alloy weld failures in service (Ref. 6) or test programs (Ref. 1-5) have occurred in the ferritic alloy. Most of the failures occurred with 2¼ Cr-1 Mo steel tubing and piping as the ferritic alloy, primarily because most fossil-fired power plants are constructed with this steel and because it was also used in most of the test programs (Ref. 1-5). Various austenitic stainless steels are used in power plants including Types 304, 316, 321 and 347. Because failure occurs in the ferritic steel, however, the austenitic stainless steels are not discussed here.

The microstructure of a typical dissimilar alloy weld failure between 2¼ Cr-1 Mo steel and austenitic stainless steel steam pipe has been studied by a number of investigators (Ref. 1-15), and factors that contribute to dissimilar alloy weld failure have long been understood (Ref. 1-5). Tucker and Eberle (Ref. 4) summarized them as:

1. Cyclic thermal stresses.
2. Low oxidation resistance of the low-alloy ferritic steel.
3. Carbon migration.
4. Metallurgical deterioration caused by elevated temperature service.

Although several reasons for dissimilar alloy weld failures have been postulated (Ref. 2-5), no comprehensive mechanism for relating microstructure to failure has been given. This paper presents thoughts on the subject that are based on our observations on experimental welds and on failed and unfailed welds taken from fossil-fired plants as well as on observations by other investigators.

Based on paper presented at the 61st AWS Annual Meeting held in Los Angeles, California, during April 13-18, 1980.

R. L. KLUEH and J. F. KING are with the Metals and Ceramics Division of the Oak Ridge National Laboratory, Oak Ridge, Tennessee.

Experimental Procedure

Optical metallography was used as the primary technique in this study. Several failed and unfailed dissimilar-alloy weld joints that had been in service for as long as 137,000 hours (h) in fossil-fired steam plants were obtained. Also, several bead-on-plate welds were made on 2¼ Cr-1 Mo steel plate by the gas tungsten arc process with Type 309 stainless steel, ENiCrFe-2, ENiCrFe-3, and ERNiCr-3 filler metals. Parts of these bead-on-plate welds were examined in the as-welded condition, but others were examined after thermally aging or after a postweld heat treatment.

Selected specimens were also studied in more detail with the electron microprobe.

Results and Discussion

The microstructure of the dissimilar alloy weld is determined by phases developed during welding. Various phases are indicated in Fig. 1 which consists of Fe-Ni-Cr diagrams taken from the *Metals Handbook* (Ref. 16) on which regions representing Type 309 stainless steel and nickel-rich filler metals have been superimposed.

Recognizing the phases that can form when 2¼ Cr-1 Mo steel is welded with

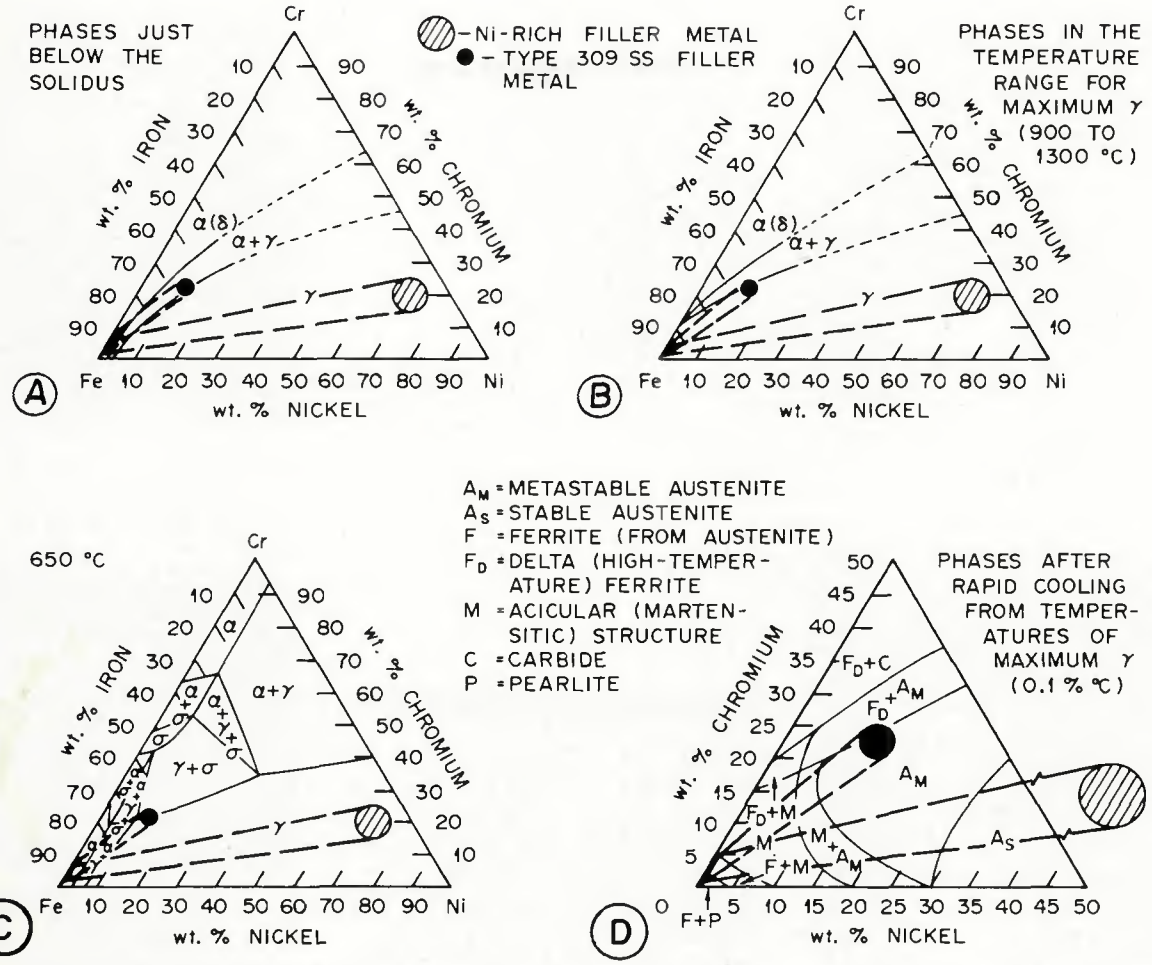

Fig. 1—Sections of ternary Fe-Ni-Cr phase diagram. Regions are shown to represent the compositions of 2¼ Cr-1 Mo steel, Type 309 stainless steel filler metal, and the typical nickel-base filler metal. Published by permission of American Society for Metals, E. C. Bain and R. H. Aborn, "Cr-Fe-Ni Phase Diagrams," pp. 1260-61 in **Metals Handbook,** *Cleveland, 1948*

different filler metals, discussion that follows below centers on actual microstructures that develop in dissimilar alloy welds during welding, when aged in the laboratory, and during elevated temperature service. Finally, a failure mechanism is postulated on the basis of microstructural observations.

Support for the proposed mechanism is presented from metallographic studies on dissimilar alloy joints that failed during service in fossil-fired plants.

Experimental Observations

To determine what phases form during welding, we made several bead-on-plate welds on annealed 2¼ Cr-1 Mo steel plate. Figure 2 shows the interface microstructure of Type 309 stainless steel weld metal on the 2¼ Cr-1 Mo steel plate. Two observations are of interest:

1. The interface with the weld metal is very indistinct.
2. The grain boundaries in the 2¼ Cr-1 Mo steel away from the interface are parallel to the fusion line.

The latter feature is common to all such fusion welds, including welds made on steam generator tubes, as we will demonstrate. On close examination of Fig. 2, another phase appears to be present in the grain boundaries—Fig. 2 B.

The microstructures of Fig. 2 were brought out with the typical etchant for 2¼ Cr-1 Mo steel (2% nital). When the 2¼ Cr-1 Mo steel was over-etched, another zone became visible between the weld metal and the 2¼ Cr-1 Mo steel (Fig. 3) and would appear to be the "light-etching phase" observed by Eaton and Glossop (Ref. 10) and Jones (Ref. 13).

As a result of the heavy etching, we found it difficult to resolve, simultaneously, the light-etching region and the 2¼ Cr-1 Mo steel microstructure. By focusing on the light-etching region, a substructure can be delineated—Fig. 3. Furthermore, at the edge of this region (away from the weld metal), a narrow dark area occurs that is somewhat different from the region on either side of it. This region could be one that contained two phases [$\gamma + \alpha(\delta)$] during welding—Fig. 1.

When a piece of the bead-on-plate weld was given a 5 h postweld heat treatment at 704°C (1299°F), the dark-etching "lamellar phase" of Eaton and Glossop (Ref. 10) was observed—Fig. 4. All indications are that this is a precipitate that formed in the light-etching region of Fig. 3. Although difficult to resolve, at high magnification a small precipitate again appears to be present in the grain boundaries parallel to the fusion line (arrows in Fig. 4B). The microstructure between these grain boundaries and the dark-etching phase is noticeably different from that of the 2¼ Cr-1 Mo steel well away from the fusion line. Extremely few precipitate particles are in the matrix between the grain boundaries and the lamellar precipitate. The dark-etching phase also appears when a Type 309 stainless steel bead-on-plate weld is aged for 500 h at 566°C (1051°F) (without a postweld heat treatment; this aging treatment is similar to a service exposure).

Similar microstructures occur when nickel-base filler metals are used instead of Type 309 stainless steel filler metal. Figure 5A shows the interface for an ERNiCr-3 filler metal. After a piece of this weld was aged for 500 h at 566°C (1051°F), the dark-etching region again

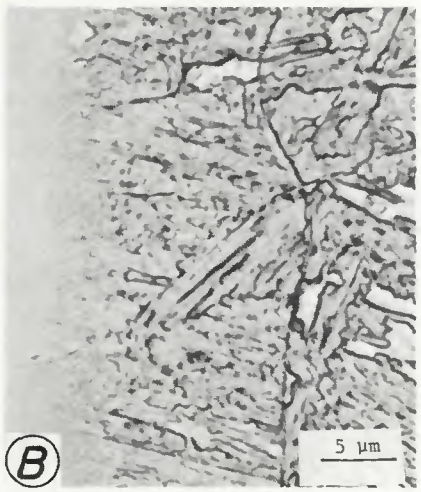

Fig. 2—Microstructure of region near fusion line of bead-on-plate weld of Type 309 stainless steel on annealed 2¼ Cr-1 Mo steel. Etched lightly with 2% nital

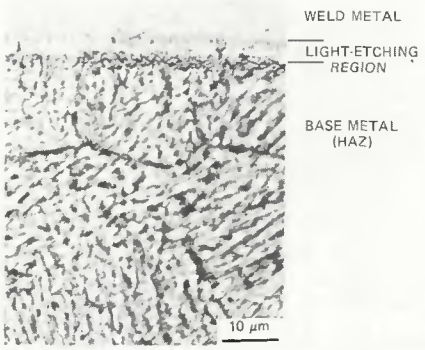

Fig. 3—Microstructure of region near fusion line of bead-on-plate weld of Type 309 stainless steel on annealed 2¼ Cr-1 Mo steel. Etched heavily with 2% nital to bring out light-etching zone

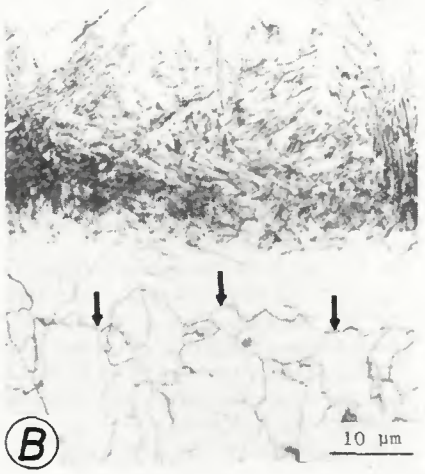

Fig. 4—Microstructure of region near fusion line of bead-on-plate weld of Type 309 stainless steel filler metal on 2¼ Cr-1 Mo steel plate annealed 5 h at 704°C (1299°F) after welding. Etched with 2% nital. Arrows indicate precipitates in grain boundaries

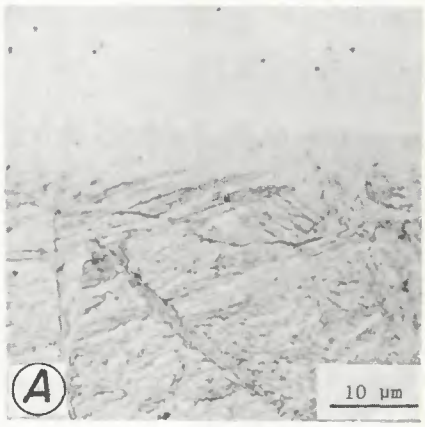

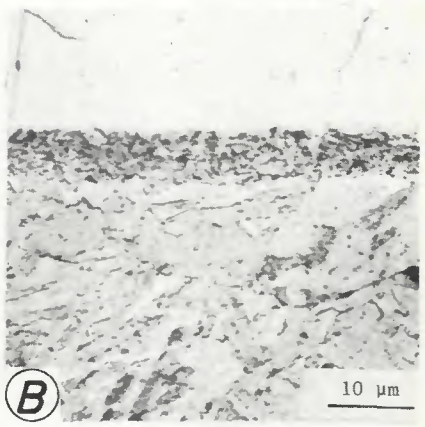

Fig. 5—Microstructure of region near fusion line of bead-on-plate weld of ERNiCr-3 filler metal on annealed 2¼ Cr-1 Mo steel plate: A—as-welded; B—aged 500 h at 566°C (1051°F)

became evident—Fig. 5B. We made similar observations on bead-on-plate welds for ENiCrFe-3 and ENiCrFe-2 on 2¼ Cr-1 Mo steel plate.

After prolonged service in a fossil-fired boiler, the microstructure changes, but vestiges of the as-welded microstructure remain; this is shown in Fig. 6 for a Type 321 stainless steel—2¼ Cr-1 Mo steel joint welded with ENiCrFe-1. This joint was in service at about 560°C (1040°F) for more than 100,000 h. Interestingly, the dark-etching phase has disappeared. The grain boundaries parallel to the fusion line are still present, and they very definitely contain another phase.

Although not easily resolved, voids or fissures were often seen to be associated with the precipitates in the parallel grain boundaries of welds that had been in service. Such fissures were also observed by Gray et al. (Ref. 6)—Fig. 7. Because they were not observed on the bead-on-plate welds (as-welded or aged), they could well be creep cavities.

Development of Microstructure

Our experimental observations can be related to the phase relationships mentioned earlier. During welding, chromium and nickel from the weld metal diffuse into the 2¼ Cr-1 Mo steel (other elements present in the weld metal will also diffuse into the 2¼ Cr-1 Mo steel but will have much less effect because of their smaller concentrations). At the fusion line, a region of melted-but-unmixed 2¼ Cr-1 Mo steel will emerge, in which this diffusion can readily occur; solid state diffusion will also be rapid at the elevated temperatures developed during welding. Because the high nickel and chromium concentrations increase the hardenability, this region will transform to martensite during cooling.

In addition to the diffusion of nickel and chromium from the weld metal, carbon will diffuse toward the weld metal. Because the driving force for this migration is provided by the higher solubility of carbon in the weld metal (this applies for both types of filler metal), the increased carbon content in the nickel and chromium diffusion zone will further increase hardenability.

Decarburization will be accompanied by carbide dissolution. The loss of carbon from the 2¼ Cr-1 Mo steel in the vicinity of the fusion line allows grain growth to occur. The grain boundaries move away from the fusion line into the 2¼ Cr-1 Mo steel, giving rise to grain boundaries that are parallel to the fusion line. Grain-

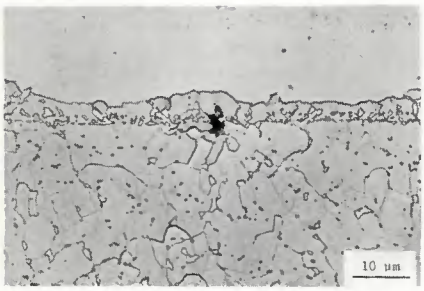

Fig. 6—Microstructure of transition weld joint between 2¼ Cr-1 Mo steel and Type 321 stainless steel welded with ENiCrFe-1. Joint was in service in a fossil-fired plant for more than 100,000 h at about 560°C (1040°F)

boundary migration is controlled by the rate of decarburization; the distance of these boundaries from the fusion line indicates the size of the decarburized region (grain-boundary migration may be controlled by the carbide dissolution).

We postulate that, in accordance with the phase diagram (Fig. 1), the former weld metal will be austenitic. The diffusion zone (formerly base metal) that is high in nickel and chromium solidifies to and transforms to martensite on cooling. Because the region is higher in carbon as a result of diffusion from the 2¼ Cr-1 Mo steel, the precipitate that forms in this region when tempered, or aged, is a carbide (same as the proposal by Wood—Ref. 11). The narrow dark region noted in Fig. 3 could be a region somewhat higher in chromium and therefore a two-phase $\alpha(\delta) + \gamma$ region during cooling. Farther into the HAZ of the 2¼ Cr-1 Mo steel, the transformation depends on the temperature reached during welding. Where temperatures exceed the A_{c_1}, γ forms; when cooled, γ transforms to bainite or proeutectoid ferrite. When heated below A_{c_1}, no transformation occurs; only tempering of the untransformed base metal takes place.

The phase in the grain boundaries parallel to the fusion line (Fig. 6) is of special interest because transition joint failures usually occur by cracks that propagate along this boundary or in a region adjacent to it (Ref. 6, 11).* High-chromium δ-ferrite regions are believed to form in these grain boundaries during welding. Apblett et al. (Ref. 18) showed that δ-ferrite can occur in 2¼ Cr-1 Mo steel heated to welding temperatures. They stated, "Apparently when the carbide phase (in the annealed 2¼ Cr-1 Mo steel being heated during welding) dissociates, there exist regions of sufficiently high-alloy content to close the gamma loop." They concluded that the high-alloy content at the site of the original carbide resulted in alloy diffusion, which caused the size of the δ-ferrite regions to increase. They found these regions to occur only at grain boundaries.

During welding, the 2¼ Cr-1 Mo steel in the HAZ adjacent to the weld metal is austenitized. Because of the high temperatures in this region, carbides quickly dissociate. Homogenization and austenite grain growth are rapid, giving rise to large austenite grains immediately adjacent to the weld metal. At some distance into the 2¼ Cr-1 Mo steel, the temperature decreases to the point that grain growth slows. We believe this decrease occurs where the grain boundaries are aligned parallel to the fusion line. Under these conditions, once the carbides in these boundaries dissociate, a region rich in chromium and molybdenum (both ferrite stabilizers) is left behind.

For whatever reason (favorable surface energy, etc.), a δ-ferrite region rich in chromium and molybdenum of the type found by Apblett et al. (Ref. 18) could form within the grain boundaries and grow by grain-boundary diffusion. We would expect the regions to be especially chromium rich, because more than 4.5 times as many chromium atoms as molybdenum atoms are present in the alloy.

Because of the high-chromium concentrations these regions have a higher carburization potential. While cooling from the welding temperature and later during service, these regions will carburize, thus forming the chromium carbides that commonly occur in this alloy (molybdenum carbides are also possible). As these regions of high chromium carburize, they will grow by diffusion of chromium from the matrix immediately adjacent to the grain boundary.

Carbides in the boundaries are larger than those in the matrix and are in a low-energy position (the grain boundary). Because of this, the growth of the grain boundary carbides should be favored over those in the nearby matrix. Figure 7 shows that few precipitates occur adjacent to the grain boundary on the side away from the weld metal. The large carbides on the other side of the boundaries are usually in grain boundaries perpendicular to the fusion line. The small ones often occur in rows parallel to the grain boundaries that parallel the fusion line; they could have formed because of chromium and molybdenum concentration buildup in the grain boundary before it migrated.

To confirm the possible validity of the above hypothesis, we did microprobe studies on the ENiCrFe-1 weld on 2¼ Cr-1 Mo steel and Type 321 stainless steel that had been in service over 100,000 h in a fossil-fired boiler. In one experiment, we annealed a piece of this joint for 1 h at 927°C (1701°F) and air cooled it (a normalizing treatment for the 2¼ Cr-1

**As pointed out by Wood, the light- and dark-etching regions are interesting, but crack propagation is always outside that region.*

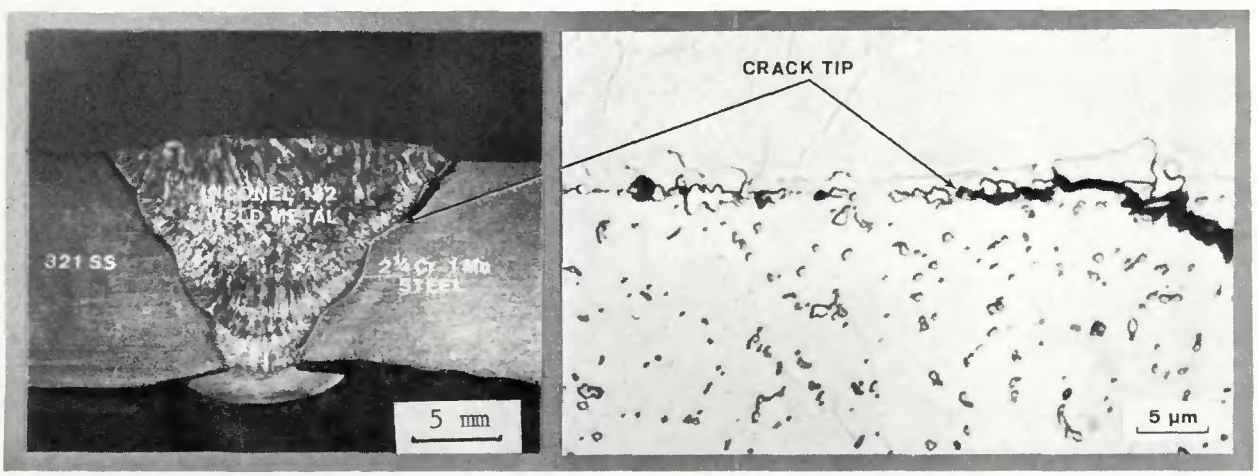

Fig. 7—Cross section of failed transition joint that was in service for about 150,000 h (17 years) at about 560°C (1040°F). The photomicrograph shows that the crack propagates in grain boundaries of 2¼ Cr-1 Mo steel. Source: Gray, R. J., King, J. F., Leitnaker, J. M., and Slaughter, G. M., **Examination of a Failed Transition Weld Joint and the Associated Base Metals.** *ORNL-5223, 1977, Oak Ridge National Laboratory, Oak Ridge, TN*

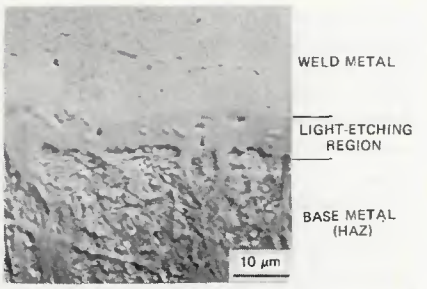

Fig. 8—Microstructure of a transition joint between 2¼ Cr-1 Mo steel and Type 321 stainless steel welded with ENiCrFe-1, in service at about 560°C (1040°F) for 100,000 h, after which it was normalized (1 h at 927°C or 1701°F, then air cooled). Differential interference contrast micrograph. Differences in hardness give rise to relief polishing. The layer between the weld metal and the 2¼ Cr-1 Mo steel is the light-etching region

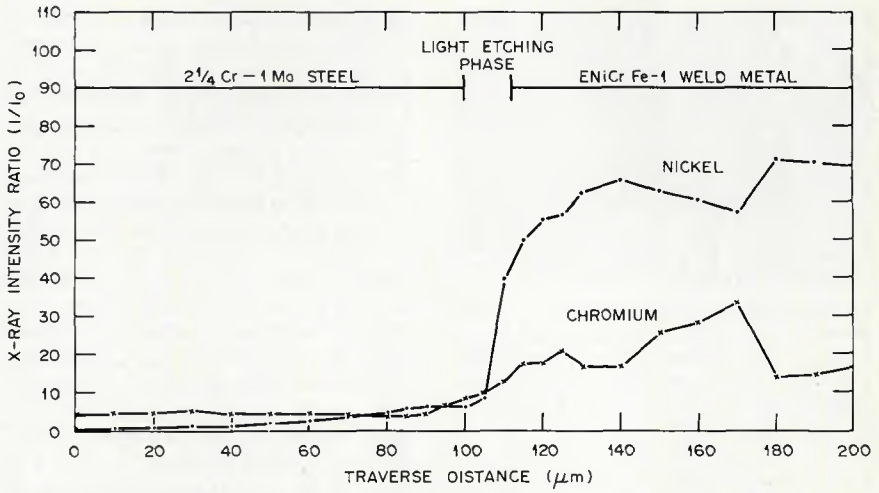

Fig. 9—Nickel and chromium profile across fusion line region of specimen in Fig. 11. Shown is the light-etching zone to be associated with diffusion from the weld metal

Mo steel). After this treatment, the light-etching phase (which we assume is martensite rich in nickel and chromium) was clearly visible—Fig. 8.

With the microprobe, nickel and chromium profiles were determined from the weld metal through the light-etching phase into the 2¼ Cr-1 Mo steel. The light-etching phase definitely delineated the region of nickel and chromium diffusion—Fig. 9. Qualitative microhardness observations showed that the light-etching region is harder than the neighboring regions.

We also examined the precipitates in the grain boundaries parallel to the fusion line of the specimens shown in Fig. 6. This was the same ENiCrFe-1 weld that had been in service more than 100,000 h at about 560°C (1040°F) but which was not heat treated before examination. We compared the x-ray intensities for three precipitates with the intensities of the nearby matrix. As shown in Fig. 10 for one of these precipitates, the chromium composition was considerably higher than it was in the adjacent matrix. A slight increase also occurred in the molybdenum concentration. The other two precipitate particles showed similar results. These microprobe results are in agreement with the proposed mechanism.

We also had access to an induction-pressure weld between 2¼ Cr-1 Mo steel and Type 321 stainless steel, which failed in service after about 137,000 h at about 560°C (1040°F). These welds are made by induction heating the tubes to temperatures near 1200°C (2192°F) and forcing the tubes together.

The microstructure in this case was somewhat different from that observed for fusion welds—Fig. 11. The decarburized grain-growth region was readily apparent. In addition to the decarburized region, what appeared to be a two-phase zone occurred adjacent to the bond line. At high magnification the second phase appears to be similar to the phase in the grain boundaries parallel to the fusion line in the fusion welds.

We feel that the second phase is the same as the phase in the parallel grain boundaries of the fusion welds. The higher chromium concentration in the stainless steel allows chromium to diffuse into the 2¼ Cr-1 Mo steel and gives rise to a

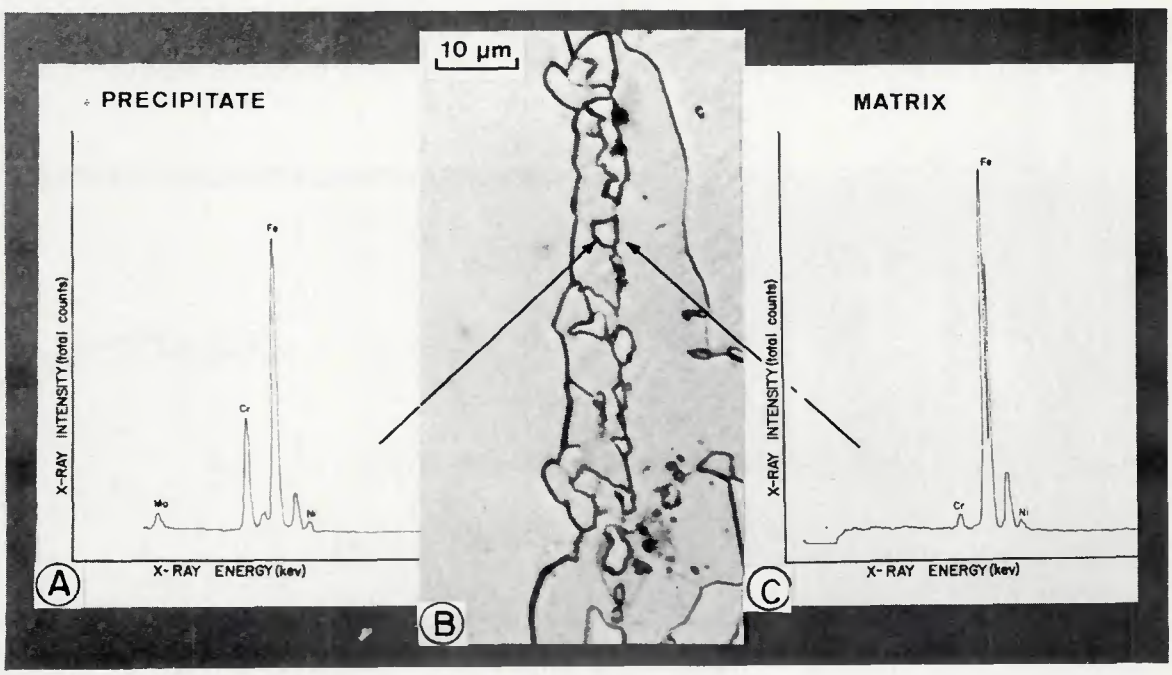

Fig. 10—X-ray intensities for precipitate and 2¼ Cr-1 Mo steel matrix for the transition joint in service for more than 100,000 h at 560°C (1040°F)

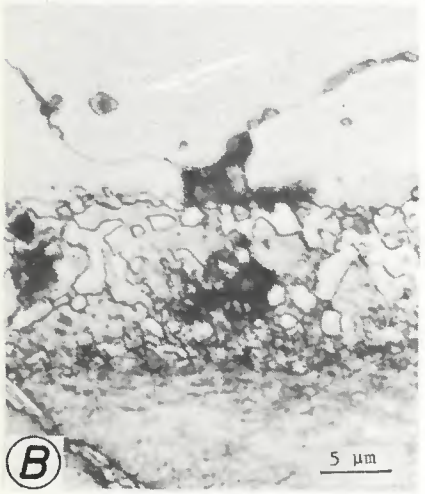

Fig. 11—Microstructure of an induction-pressure weld between 2¼ Cr-1 Mo steel and Type 321 stainless steel. The joint was taken from service after about 137,000 h at about 560°C (1040°F). Etched with 2% nital

δ-ferrite + austenite region at the welding temperatures. As opposed to the single-phase diffusion region in the fusion weld, this two-phase diffusion region results because solid state diffusion occurs, whereas liquid state diffusion is postulated for the fusion weld. Microprobe studies verified that the second phase was high in chromium.

The photomicrographs (Fig. 11) also show indications of precipitate particles in the grain boundaries of the Type 321 stainless steel. This finding is attributed to carbon diffusion from the 2¼ Cr-1 Mo steel. The grain boundary microstructure of the 2¼ Cr-1 Mo steel near the interface of the pressure welds is also different from that of the fusion weld (no parallel grain boundaries)—Fig. 6.

In summary, the important new experimental information presented in this section is evidence that the grain-boundary precipitates are chromium-rich and that the chromium is depleted in the vicinity of the grain boundaries for fusion welds and adjacent to the two-phase region for the induction-pressure welds. We have suggested a mechanism by which the high-chromium regions can occur.

Fig. 12—Photomicrograph of an oxide-filled crack in failed weld joint

Failure Mechanism

As discussed earlier, dissimilar-alloy weld joints fail by the propagation of cracks parallel to the fusion line, usually at a small distance (5 to 15 μm) from the fusion line (Ref. 1, 3-6, 10-13). In the failure of fusion welds that we and other investigators (Ref. 6) have examined, it is found that the crack usually follows the grain boundaries that parallel the fusion line [the grain boundaries that contain the precipitate particles (Ref. 6)]—Fig. 7. Such cracks often contain oxides (Fig. 12), sometimes in the form of an "oxide finger" that reaches inward from the external surface.

Based on our experimental observations, we postulate a failure mechanism for dissimilar-alloy welds. We found that the high-chromium particles formed in the grain boundaries parallel to the fusion line of fusion welds deplete the chromium from the adjacent matrix. Because chromium imparts oxidation resistance to the 2¼ Cr-1 Mo steel, this region should be more susceptible to oxidation than are its surroundings.

Reduced oxidation resistance leads to an oxide notch at the external surface—Fig. 13. Such a notch is present on all tubes that have been in elevated-temperature service. Without the loss of chromium from the matrix, however, no pronounced notch should form slightly away from the fusion line, and the oxide thickness at that point should be the same as it is on 2¼ Cr-1 Mo steel away from the interface, which is not the case—Fig. 13.

Tucker and Eberle pointed out that, because of the difference in oxidation resistance between 2¼ Cr-1 Mo steel and the weld metals (all of which are high in chromium and thus more oxidation resistant than is 2¼ Cr-1 Mo steel), an "oxide notch" forms at the interface. We

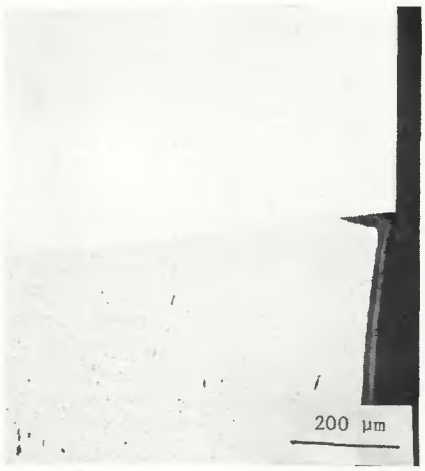

Fig. 13—Example of oxide notch formed on outer surface of a dissimilar-alloy weld joint

believe that, more important, the notch effect depends on chromium depletion in the matrix adjacent to the grain boundary. (Ref. 4) We also believe that the notch then leads to crack nucleation and propagation.

In addition to the loss of chromium from the matrix, which leads to a decrease in oxidation resistance, the carbon concentration is also depleted by diffusion to the weld metal and carbide formation in the high-chromium and molybdenum regions in the grain boundaries. Loss of carbon is accompanied by loss of strength (Ref. 7). Hence, the region is of lower strength than is the surrounding material, thus favoring stress concentration and failure in the region. Although the low-strength material has inherently high ductility, a low-ductility failure results because only a very narrow zone is involved in the failure.

Although this hypothesis can explain the observations on failure position, a crack nucleation mechanism is required—that is, some joints have operated successfully for more than 150,000 h, whereas others have failed in less than

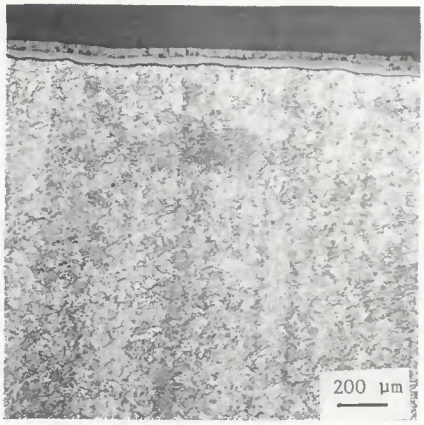

Fig. 14 — The 2¼ Cr-1 Mo steel fracture surface. Oxide forms on surface after fracture. Photomicrograph is near the inner surface. Etched with 2% nital

20,000 h (all joints develop a notch, even those that do not fail). This difference occurs for seemingly similar joints (joints that were similarly prepared and were in service under seemingly similar plant conditions). Such discrepancies occur for similar welds, regardless of filler metal (austenitic stainless steel or nickel base) or welding process (induction-pressure weld or fusion weld). The question then becomes: Why does a crack nucleate below the oxide notch in some cases and not in others?

Given supposedly similar operating conditions (temperature, number of thermal cycles, and internal tube pressure), the only possible difference from one joint to another must involve stresses from external loading conditions (i.e., stresses on the tubes as a result of the design and construction, including welding stresses but excluding stresses from the internal steam pressure). Such loads are known to be present, although their nature and position are not well documented.

We propose that some critical external stress is necessary to nucleate a crack at the oxide notch: if the external stress is large enough, it alone could nucleate the crack. However, the total stress from the external load superimposed on the cyclic thermal stresses (generated by differences in thermal coefficients of expansion for the joint materials, as well as the internal steam pressure) more probably leads to crack nucleation at the notch. The crack is probably a fatigue crack nucleated by the combined external and cyclic stresses. The cycles are those engendered by startups and shutdowns of the power plant (several hundred usually occur during 100,000 h of operation). The idea of a fatigue crack is further substantiated by the fact that thermal cycling is required to produce failure in the laboratory (Ref. 5). Under this proposal, only joints that are stressed by external loads above some critical value will nucleate a crack and fail.

Once a crack is nucleated, crack growth will proceed from the influence of the external stress, from the cyclic thermal stresses, and possibly from the stresses generated by the oxide that forms within the crack. Because the region adjacent to the grain boundaries parallel to the fusion line has low oxidation resistance, a tendency for oxidation to continue along this boundary will exist. Once a crack forms ahead of the oxide notch, oxide should quickly fill the crack — Fig. 12.

Assuming the oxide is magnetite (Fe_3O_4), as is normally the case for 2¼ Cr-1 Mo steel, the volume ratio of the oxide to metal is much greater than unity. For iron, the ratio is 2.10 (Ref. 19). Thus, the oxide formed in this crack could itself generate stresses and hasten failure. These stresses, added to those imposed by thermal cycling and by external loads, would then give rise to crack propagation and failure. It should also be noted that crack propagation along the parallel grain boundaries will be aided by any creep cavities that may have formed adjacent to the precipitates.

The proposed mechanism appears to describe fusion weld failures adequately. Although only a limited number of induction-pressure welds were examined, we showed previously that the microstructures of these are different from those for the fusion welds (there are no grain boundaries parallel to the fusion line). Nevertheless, we believe that a similar mechanism applies for the induction-pressure welds. Based on studies of several failed induction-pressure welds, our observations further substantiate the proposed failure mechanism.

In induction-pressure welds, chromium is removed from the 2¼ Cr-1 Mo steel matrix adjacent to the two-phase zone described — Fig. 11. On close examination, an almost continuous layer of this phase appears to exist at the interface of the two-phase region and 2¼ Cr-1 Mo steel. During service, this phase could grow by the same method as the particles in the grain boundaries of the fusion weld. An oxide notch is always observed to form in this chromium-depleted region.

Because of the high temperatures and relatively long times involved in making an induction-pressure weld, decarburization and grain boundary migration are much more extensive for these welds. Many of the boundaries are almost perpendicular to the fusion line. Because of the high temperatures, the carbides in these boundaries could form by the mechanism postulated for those in the grain boundaries of the fusion welds. Regardless of how they form, numerous precipitates occur in the grain boundaries, but very few in the matrix. Thus, chromium again appears to be drained from the matrix as shown by electron microprobe studies.

We did a detailed failure analysis of an induction-pressure weld between Type 347 stainless steel and 2¼ Cr-1 Mo steel. This joint was from an oil-fired plant that had operated about 20,000 h and had been cycled 385 times (40 cold starts). The operating temperature for this unit ranges from 525 to 550°C (977 to 992°F). We also obtained an unfailed joint that had been in service immediately adjacent to the failed joint. A discussion of this failed joint is of interest because it failed in a manner that would be expected if our proposed mechanism (from the standpoint of chromium depletion) is correct.

When the failed joint was cut from the unit, it fell apart. From a close visual examination we found that most of the fracture surface was smooth — as if the tube separated at the weld interface. However, near the tube outside surface, a region occurred in which material from the 2¼ Cr-1 Mo steel adhered to the surface of the Type 347 stainless steel.

Metallographic examination of two sections from the failed tube indicated that most of the separation occurred at or near the prior weld interface — Fig. 14. The separation at the weld interface occurred from the tube inner surface through about 85 to 90% of the wall thickness. For the remainder of the wall thickness, separation occurred along 2¼ Cr-1 Mo steel grain boundaries about one grain width into the 2¼ Cr-1 Mo steel. This separation resulted in grains of 2¼ Cr-1 Mo steel adhering to the Type 347 stainless steel (Fig. 15) and grains pulling from the 2¼ Cr-1 Mo steel (Fig. 16). Interspersed within the grain-boundary separation, further regions occurred in which separation again occurred along the weld interface.

The first metallographic examination of the cross section of the unfailed joint revealed no indication of cracks forming parallel to the weld interface. Features of interest in the unfailed joint were the oxide notches that appeared on the external surfaces at the weld interface. Two types were observed: a wedge-shaped notch at the inner surface (Fig. 17A) and a blocky notch at the outer surface (Fig. 17B). Similarly shaped notches were observed on both pieces of the joint that were examined.

When etched, the interface microstructure of the unfailed specimen was similar to the uncracked regions of the joint discussed earlier — Fig. 11. The width of this zone was somewhat less than that of the other weld. This difference probably reflects the different service time (20,000 vs. 137,000 h), which results in differing amounts of mass transfer. The wedge-shaped notch at the inner surface forms along the weld interface, as we would expect for this chromium-depleted zone. The blocky notch was somewhat more complicated.

A detailed examination was made to

Fig. 15—Fracture surface showing grains of 2¼ Cr-1 Mo steel adhering to Type 347 stainless steel. Photomicrograph is near the outer surface. Etched with aqua regia

Fig. 16—Fracture near outer surface showing that 2¼ Cr-1 Mo steel grains were removed during fracture. Etched with 2% nital

verify that failure was not the result of a defective weld. Although details of that examination are not discussed here, we concluded that metallic bonding was achieved during welding and that failure was of the dissimilar-alloy type.

After grinding and repolishing the unfailed specimen, we found evidence of crack formation. On the tube inner surface of both metallography specimens (the same two pieces of sample were studied), we found evidence that a crack was present—Fig. 18. Figure 18 shows the oxide wedge and a very fine "crack" ahead of the massive wedge. As expected, the cracks run along the weld interface adjacent to the two-phase zone. It is not possible to determine whether or not the crack contains oxide, although it appears to.

Examination of the blocky outer surface oxide notch also provided additional evidence of the failure mode (Fig. 19). Two cracks are evident within 2¼ Cr-1 Mo steel grain boundaries. The crack adjacent to the oxide layer contains oxide, but we are less certain that the other does. These cracks come through 2¼ Cr-1 Mo steel and move toward the weld interface.

From these observations this unfailed joint appears to be in the early stages of failure. The fracture morphology of the failed specimen can now be readily explained. Cracks are nucleated at both oxide notches. At the inner surface the crack propagates along the two-phase zone, as expected, because it is a chromium-depleted zone. However, at the outside surface, cracks nucleate and propagate in grain boundaries in the 2¼ Cr-1 Mo steel adjacent to the bulky oxide notch. When the joint fails, the fracture surface is smooth and flat near the inner surface and tears grains from the 2¼ Cr-1 Mo steel at the outer surface.

We understand the reason for the different fracture morphology at the outer surface when we consider the welding process. Induction heating is used to heat the tubes to temperatures as high as 1200°C (2192°F). The outer surface reaches the highest temperature, probably much higher than does the inner surface (the grain sizes attest to that). At temperatures near 1200°C (2192°F), Apblett et al. (Ref. 18) noted δ-ferrite formation in grain boundaries. Thus, the δ-ferrite forms in grain boundaries near the outer surface, which leads to high-chromium concentrations at these grain boundaries. Chromium carbides eventually form, further depleting the matrix adjacent to the grain boundaries. Crack propagation occurs along these grain boundaries for the same reason that it occurs along the grain boundaries of the fusion weld. The blocky oxide at the outer surface (rather than a wedge) occurs because of the lower chromium concentration in the matrix (the chromium is in grain-boundary carbides), which is again the result of the high temperature reached by induction heating.

The short service duration (20,000 h) before failure emphasizes the importance of the thermal cycles. Previous failures of induction-pressure welds were on joints that had generally operated for 100,000 h or more (Ref. 20). However, these joints had endured considerably fewer thermal cycles than the 385 of the current joint. For example, although the other induction-pressure weld we examined (Fig. 11) was in service for over 137,000 h, it had endured only 220 cycles.

These effects of thermal cycles on failure support the formation of a fatigue crack, as proposed above: nucleation and propagation of such cracks are determined by the number of cycles and stresses in a complicated manner. Generally, for a fatigue crack to nucleate, a threshold stress needs to be exceeded; this again emphasizes the importance of the external stress on the process.

Recommendations for Improved Transition Joints

Assuming that the proposed failure mechanism is correct, we now consider how transition-joint lifetimes can be extended. Our studies indicated that, for fusion welds, the same basic metallurgical processes occur near the fusion line in the 2¼ Cr-1 Mo steel regardless of the weld filler metal used. Only the extent of the process (the amount of decarburization, etc.) is different.

The studies by Tucker and Eberle (Ref. 4) showed that the high-nickel filler metals are superior to the austenitic stainless steel filler metals. This conclusion is accepted by most people in industry, and high-nickel filler metals are now used almost exclusively. Although the microstructure at the interface of the joints made with high-nickel filler metals is similar to that of those with austenitic stainless steel filler metals, an improvement results because there is a smaller difference in coefficients of thermal expansion for the high-nickel filler metal and the 2¼ Cr-1 Mo steel than there is for the stainless steel filler metal and 2¼ Cr-1 Mo steel. This smaller difference gives rise to smaller thermal stresses. With smaller

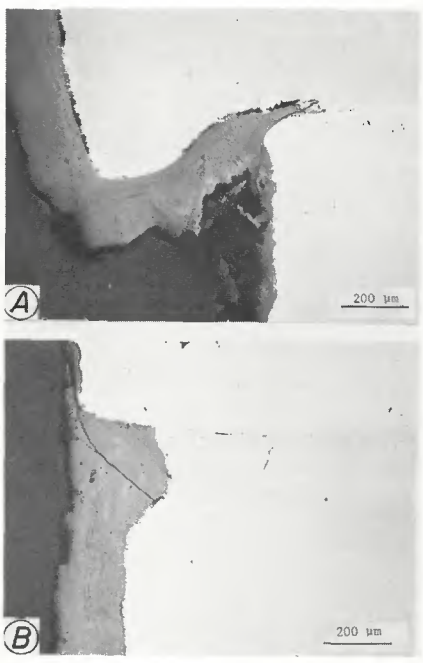

Fig. 17—Photomicrographs of oxide notches at the weld interface: A—wedge-shaped notch at the tube inner surface; B—Blocky notch at tube outer surface

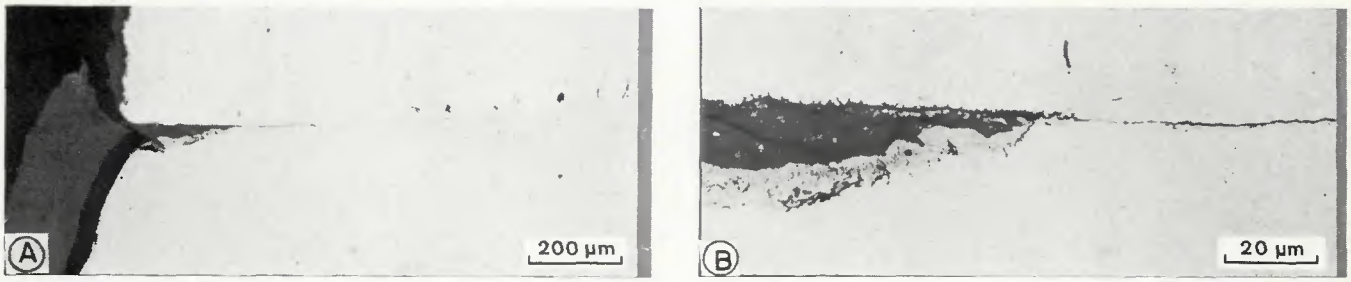

Fig. 18—After repolishing there was evidence of a crack below the wedge-shaped oxide notch of the unfailed joint

thermal stresses, larger external loads will be needed to nucleate a crack at the oxide notch.

The most obvious solution to the dissimilar-alloy weld joint problem is the minimization of external loads on the transition joint. If the external load is below that required for crack nucleation, no failure should occur. This solution has been obvious to most people. Because all external loads cannot be eliminated, it may be possible to determine which joints in a plant carry significant external loads. Periodic examination of these joints could be planned, and emergencies could be avoided by replacing these joints when inspection indicates that problems exist. Knowledge of the externally loaded joints could then be used to minimize inspection of all joints in a given plant. In future power plants, the design of the plant could provide for such a maintenance plan. Wherever possible, plant design should locate the externally loaded joints in areas in which they can be easily inspected and, when necessary, easily replaced.

Another possibility is the introduction of a transition or spool piece between the ferritic steel and the austenitic stainless steel tubes (Ref. 21). A transition piece is chosen to have a coefficient of thermal expansion that is intermediate between the ferritic and austenitic steels. This results in a more gradual change in the difference in coefficients of thermal expansion and a consequent decrease in the cyclic thermal stresses. Alloy 800H has been proposed as a transition piece for Liquid-Metal Fast-Breeder Reactor applications (Ref. 21). The improvement in thermal stresses generated in such a trimetallic joint over the bimetallic joint has been demonstrated by finite-element analysis (Ref. 22).

Other transition pieces considered include stabilized and low-carbon 2¼ Cr-1 Mo steels. The objective for using such joints was to minimize carbon transfer. As seen above, chromium depletion appears to affect adversely the operation of transition joints. For that reason it may be advisable to use a chromium-molybdenum steel transition piece with a higher chromium concentration (3 to 5% Cr or perhaps a stabilized 3 to 5% Cr alloy). In addition to keeping sufficient chromium available and thus avoiding oxide-notch formation, the larger chromium concentration would also lower the amount of carbon transferred during welding and service.

For fossil-fired plants having thousands of dissimilar-alloy weld joints, a transition piece solution might be quite expensive. Furthermore, such a joint replaces one weld by two. Because welds are critical areas in every structure and failure can occur for many reasons other than the one discussed here, a transition piece may be less than the ideal solution. However, such a solution might be possible for the joints known to have high external loads, especially if relatively few such welds are present in a plant.

Offhand, a change in welding process or procedure does not appear to offer much possibility for dissimilar-weld joint improvement. All the currently favored weld filler metals form similar microstructures at the fusion line. If it were possible to eliminate decarburization at the interface, the joint could be improved. Any joining process for which prolonged heating can be avoided should be an improvement. Obviously, the microstructures developed when induction-pressure welds are made (Fig. 12) indicate that prolonged heating is not avoided in that process. Although friction welding may be possible, this technique involves severe local heating, which would probably transfer the failure from tens of micrometers from the fusion line to only a few micrometers away. Indeed, it might aggravate the problem by narrowing the zone for which chromium is depleted.

Finally, if the formation of an oxide notch could be prevented, the life of transition joints should be extended. The most obvious way to do this would be an oxidation-resistant cover over the weld on the inner and outer surfaces of the tube. This obvious solution was proposed by Tucker and Eberle (Ref. 4). Indeed, they tested coatings applied by calorizing and chrome plating. However, when these joints were tested under cyclic conditions, the thermal expansion differences between the coatings and the other materials caused the coatings to crack, after which failure occurred by the usual manner. They did find that, "The weld overlay deposited with 80Ni20Cr withstood over 5000 h at 1100°F (2012°F), involving 308 temperature-stress cycles without notch or crack for-

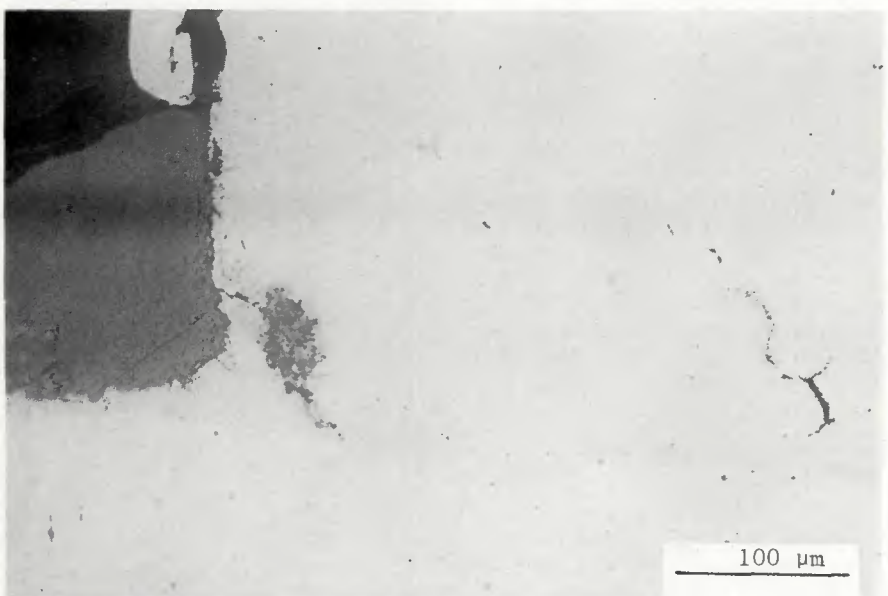

Fig. 19—Blocky-shaped oxide notch at the outer surface showing grain boundary cracks in 2¼ Cr-1 Mo steel

mation at the weld overlay-base metal junction or at the protected junction."

According to the Tucker and Eberle criteria for a successful transition joint (Ref. 4), ". . . only those specimens completing the thermal-cycling tension tests for 5000 h at the test temperature without defect were considered satisfactory." Therefore, this coating was successful; Tucker and Eberle suggested its use "as a method of emergency repair."

These results make the idea of using an oxygen barrier to prevent failure appear to have merit. Since 1956 there have been improvements in coating techniques that may offer promise. Although it was beyond the scope of this paper to search for such a barrier, any experimental program designed to improve dissimilar-weld joints should include a search for suitable oxygen barriers.

Conclusion

We have examined the dissimilar-alloy weld failure problem that is quite common in fossil-fired boilers for transition joints between ferritic steels (primarily 2¼ Cr-1 Mo steel) and austenitic stainless steels. Previous studies were reviewed. The complex microstructure that develops at a weld metal-2¼ Cr-1 Mo steel interface during welding and elevated-temperature service was examined in the as-welded, as-welded-and-tempered, and as-welded-and-aged conditions and in failed and unfailed joints that had been in service in fossil-fired boilers for more than 100,000 h. Failed induction-pressure welds were also examined. Failure generally occurs in the HAZ of the ferritic steel about 5 to 15 μm from the fusion line.

Our observations were combined with previous results to develop a theory of the mechanism by which the interface microstructure forms during welding, how it evolves during elevated-temperature service, and how this microstructure leads to failure. The chief new feature of this proposed mechanism, the formation of a chromium-depleted region, was demonstrated experimentally. We found this chromium-depleted region to be prone to preferential oxidation and eventually to lead to notch formation, crack nucleation, and propagation.

Based on the proposed failure mechanism, several possible solutions were proposed. Elimination of external loading stresses is the most obvious. Others include transition pieces (spool pieces) between the tubes to lower the thermal stresses and oxidation-resistant coatings on the external surfaces of the welds.

Acknowledgments

Special thanks are due to several people. Samples from operating fossil-fired plants were obtained from P. Haas of American Electric Power, S. Lyons of United Illuminating, and S. Hilton of the Tennessee Valley Authority. C. W. Houck performed the metallography. Detailed discussions about the manuscript with R. W. Cooper were helpful; the manuscript was also reviewed by C. J. Long, C. R. Brinkman, and G. M. Slaughter. Irene Brogden edited the manuscript, and Denise Campbell typed the final copy.

Research sponsored by the Division of Reactor Research and Technology, U.S. Department of Energy, under contract W-7405-eng-26 with the Union Carbide Corporation.

References

1. Blaser, R. V., Eberle, F., and Tucker, J. T. 1950. Welds between dissimilar alloys and full size steam piping. *Am. Soc. Test. Mater. Proc.* 50:789-807.

2. Lien, G. E., Eberle, F., and Wylie, R. D. 1954. Results of service test program on transition welds between austenitic and ferritic steels at the Phillip Sporn and Twin Branch plants. *Trans. ASME* 76:1075-1083.

3. Emerson, R. W., Jackson, R. W., and Dauber, C. A. 1962. Transition joints between austenitic and ferritic steel piping for high temperature steam service. *Welding Journal* 41(9):385-s to 393-s.

4. Tucker, J. T., and Eberle, F. 1956. Development of a ferritic-austenitic weld joint for steam plant applications. *Welding Journal* 35(11):529-s to 540-s.

5. Barford, J., and Probert, K. S. 1972 (Sept. 17-21). Interfacial Effects in Dissimilar Steel Joints. Paper presented at the International Conference on Welding Research Related to Power Plants, Marchwood Engineering Laboratories.

6. Gray, R. J., King, J. F., Leitnaker, J. M., and Slaughter, G. M. 1977 (January). *Examination of a failed transition weld joint and the associated base metals.* ORNL-5223. Oak Ridge, Tennessee: Oak Ridge National Laboratory.

7. Klueh, R. L. 1974. The effect of carbon on 2.25 Cr-1 Mo steel (I), microstructure and tensile properties. *J. Nucl. Mater.* 54, 1974, pp. 41 to 54.

8. Baker, R. G., and Nutting, J. 1959. The Tempering of 2¼ Cr-1 Mo Steel After Quenching and Normalizing, *J. Iron Steel Inst.* (London), 192, 1959, pp. 257 to 268.

9. Klueh, R. L. 1977. The Thermal Aging of Annealed 2¼ Cr-1 Mo Steel, *Environmental Degradation of Engineering Materials,* Virginia Polytechnic Institute, Blacksburg, Va., 1977, pp. 643 to 651.

10. Eaton, N. F., and Glossop, B. A. 1969. "The Welding of Dissimilar Creep-Resisting Ferritic Steels," *Met. Constr. Br. Weld. J.* suppl. 12:6-10.

11. Wood, D. 1969. Discussion session 4, welding dissimilar metals. *Met. Constr. Br. Weld. J.* 1, suppl. 12:134-136.

12. Barford, J. et al. 1970. Weldment cracking involving a complex creep-resistant steel. *Proceedings of conference on welding creep-resistant steels: 54-65 Abington, England: The Welding Institute.*

13. *Jones, W. K. C. 1974. Heat treatment effect on 2CrMo joints welded with a nickel-base electrode. Welding Journal* 53(5):225-s to 231-s.

14. Boniszewski, T. 1970. Discussion *Proceedings of conference on welding creep-resistant steel:* 185 to 186. Abington, England: The Welding Institute.

15. Glossop, B. A., Hall, D., and Irvine, J. 1969. The welding of high-pressure pipework for the CEGB. *Proceedings of conference on pipe welding:* 125-130. Abington, England: The Welding Institute.

16. Bain, E. C., and Aborn, R. H. 1948. Cr-Fe-Ni phase diagrams. *Metals handbook:* 1260 to 1261. American Society for Metals, Cleveland, Ohio.

17. Clark, J. B., and Rhines, F. N. 1959. Diffusion layer formation in ternary alloys. *Trans. ASM* 51:199 to 219.

18. Apblett, Jr., W. R., Dunphy, R. P., and Pellini, W. S. 1954. Transformation of Cr-Mo steels during welding, *Welding Journal* 33(1):57-s to 64-s.

19. Kubaschewski, O., and Hopkins, B. E. 1962. *Oxidation of metals.* London: Academic Press.

20. Personal communication from S. Hilton, Tennessee Valley Authority, Chattanooga, Tenn., July 8, 1979.

21. King, J. F., Sullivan, M. D., and Slaughter, G. M. 1977. Development of an Improved Stainless Steel to Ferritic Steel Transition Joint. *Welding Journal* 56(11):354-s to 358-s.

22. Dalcher, A. W., Yang, T. M., and Chu, C. L. 1977. High-Temperature Thermal-Elastic Analysis of Dissimilar Metal Transition Joints, *J. Eng. Mater. Technol.* 99:65-69.